European Journal of Pharmaceutical Sciences 130 (2019) 225–233

Contents lists available at ScienceDirect

European Journal of Pharmaceutical Sciences

journal homepage: www.elsevier.com/locate/ejps

Investigation of different targeting decorations effect on the radiosensitizing efficacy of albumin-stabilized gold nanoparticles for breast cancer radiation therapy

Amirhosein Kefayat[a], Fatemeh Ghahremani[b], Hasan Motaghi[c], Masoud A. Mehrgardi[c,*]

[a] Department of Oncology, Cancer Prevention Research Center, Isfahan University of Medical Sciences, Isfahan 81746-73461, Iran
[b] Department of Medical Physics and Radiotherapy, Arak University of Medical Sciences, Arak 38481-76941, Iran
[c] Department of Chemistry, University of Isfahan, Isfahan 81746-73441, Iran

ARTICLE INFO

Keywords:
Tumor targeting
Gold nanoparticles
Radiation therapy
Radiosensitizing
Smart targeting

ABSTRACT

Gold nanoparticles (GNPs) radiosensitizing effect strongly depends on the tumor targeting efficacy. The aim of this study is to identify the most ideal targeting decoration for BSA-GNPs according to tumor targeting and biodistribution. Therefore, three well-known targeting agents (folic acid, glucose, and glutamine) were utilized for BSA-GNPs decoration. Glucose-BSA-GNPs, glutamine-BSA-GNPs, and folic acid-BSA-GNPs were synthesized and then, characterized by Fourier-transform infrared spectroscopy and UV-Spectrometry. Then, the GNPs were intravenously injected 10 mg/kg to 4T1 breast tumor-bearing mice to evaluate biodistribution and radiosensitizing effects. Folic acid and glutamine decorations could significantly increase tumor targeting efficacy of BSA-GNPs as 2.1 and 2.4 times increase of gold accumulation was detected in comparison with BSA-GNPs. They exhibited the highest radiosensitizing efficacy and caused about 33% decrease in tumors volume in comparison with BSA-GNPs after 6 Gy radiation therapy. All the GNPs were completely biocompatible. Although, glutamine-BSA-GNPs and folic acid-BSA-GNPs could significantly enhance the tumor targeting and radiosensitizing efficacy of BSA-GNPs, did not exhibit any significant advantage over each other. Therefore, glutamine and folic acid decoration of BSA-GNPs can significantly increase the tumor targeting and therapeutic efficacy as radiosensitizer.

1. Introduction

Cancers' main characterization is uncontrolled and irregular cells' proliferation and growth (Wessler et al., 2017; Su et al., 2014). Radiation therapy (RT) is a common cancer treatment approaches for both curative and palliative intents. RT mechanism is irradiation with high-energy radiation beams to destroy intracellular components (Baskar et al., 2012). However, tumor's radioresistance causes RT failure and consequent tumor relapse, especially for solid tumors. One potential solution is the increase of local energy deposition at the tumor and sparing surrounding normal tissues which can be achieved by radiosensitizers (Malik et al., 2016). Radiosensitizers are agents which make tumor cells more susceptible to RT (Brown et al., 2017).

Gold ($Z = 79$) is a promising radiosensitizer and gold nanoparticles (GNPs) offer many advantages over other GNPs including small size (1–100 nm), ability to evade the immune system, and preferential tumor targeting (Butterworth et al., 2012). Bovine serum albumin (BSA) is a well-known capping agent for GNPs synthesis (Murawala et al., 2014; Jain et al., 2011; Tse et al., 2017). BSA capped GNPs (BSA-GNPs) are significantly biocompatible, stable, and exhibit considerable cancer cell uptake (Khullar et al., 2012; Singh, 2017; Miranda et al., 2016; Mocan et al., 2015). Also, BSA-GNPs have received lots of attention in cancer treatment due to their functionalizing ability with various targeting agents according to BSA structure and active groups. GNPs targeting decorations are very determinative in their efficacy (McQuaid et al., 2016; Haume et al., 2016). Although many different targeting decorations for GNPs have been investigated, there is no comprehensive study to identify the most ideal targeting decoration for tumor. Efficient tumor targeting can enhance the therapeutic ratio by achieving a greater nanoparticle concentration within the tumor, but also decrease normal organ toxicities. Many tumor targeting agents have been announced which can significantly affect the GNPs efficacy and properties (Nicol et al., 2015; Schuemann et al., 2016).

Recently, some targeting agents like glucose, glutamine, and folic acid have received lots of attention (Pavlova Natalya and Thompson Craig, 2016; Patil et al., 2016). Folic acid (FA) receptor is highly

* Corresponding author.
E-mail address: m.mehrgardi@chem.ui.ac.ir (M.A. Mehrgardi).

https://doi.org/10.1016/j.ejps.2019.01.037
Received 11 October 2018; Received in revised form 11 January 2019; Accepted 30 January 2019
Available online 31 January 2019

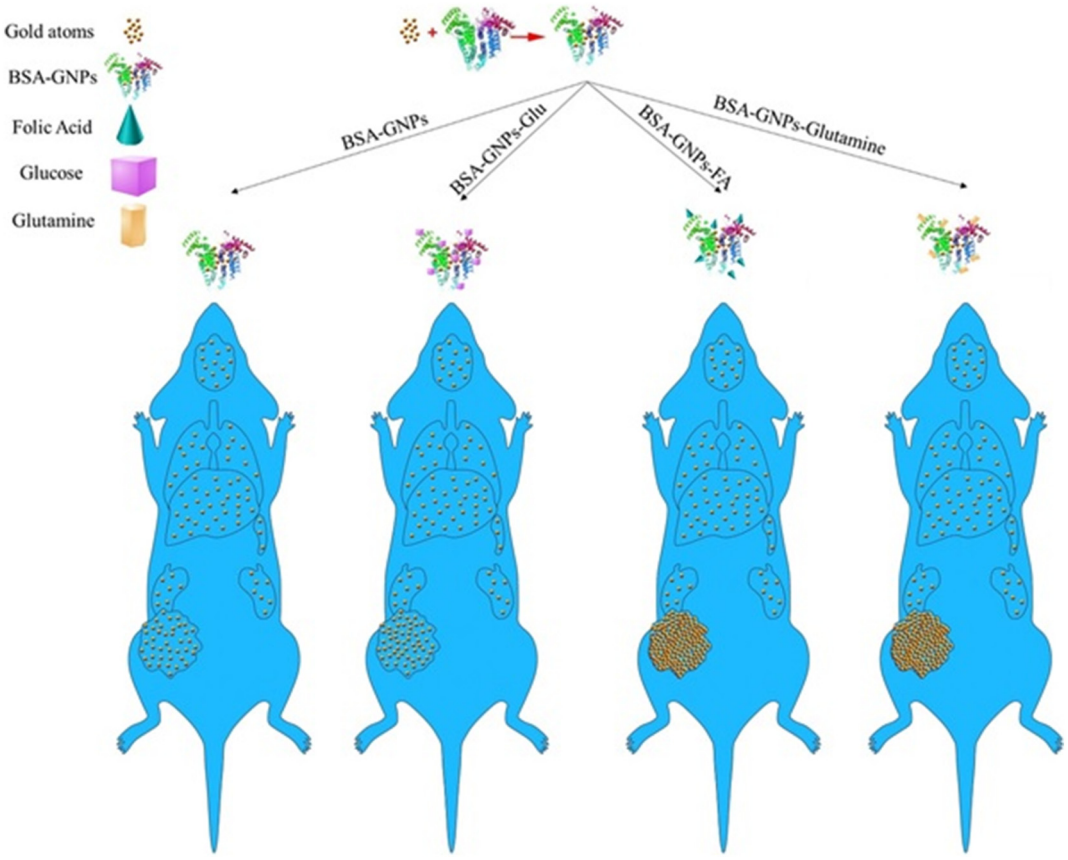

Fig. 1. Tumor accumulation is the main determinative factor for GNPs radiosensitizers' efficacy. Therefore, different decoration of BSA-GNPs was synthesized and their tumor targeting efficacy was evaluated in 4T1 breast tumor-bearing mice.

overexpressed in many cancers like breast (Hartmann et al., 2007), ovary (Toffoli et al., 1997), lung, and colon. In addition, some other properties like small size and structural stability for a broad range of temperatures and pH, making it a good candidate as a targeting agent. FA attaches to its receptors and cells starts to internalize the receptor-FA complex plus its attached cargo *via* endocytosis (Reddy and Low, 1998; Zwicke et al., 2012).

Cancer cells are highly active metabolic cells. According to the Warburg effect, they have extremely elevated glycolysis and exhibit increased glucose dependency (Vander Heiden et al., 2009). The active uptake of glucose by cancer cells is significantly more than normal cells due to the extensive expression of glucose uptake pumps like GLUT-1 (Younes et al., 1997). This obvious fact constitutes the basics of 18-fluorodeoxyglucose-positron emission tomography (FDG-PET) used in clinical diagnose of cancer (Hamanaka and Chandel, 2012; Maddalena et al., 2015; Venturelli et al., 2016). Glutamine is a non-essential amino acid and a key ingredient of cell culture medium to support cancer cells growth. Many pieces of evidence demonstrate glutamine role as a major cellular respiratory fuel. The mitochondria use glutamine as a suitable substrate for oxidation and to generate the metabolic intermediates required for the cell growth (Ko et al., 2011). Cancer cells as avid glutamine consumers compete with the host normal cells for circulating glutamine (Wise and Thompson, 2010). Even, glutamine is more necessary than glucose for cancer cells. Many studies introduce tumors as “glutamine traps” and cause glutamine deficiency for the other body organs (Wise and Thompson, 2010; Lu et al., 2010).

BSA-GNPs are well-known radiosensitizers for cancer RT. However, the main challenge is optimizing their efficacy. Although different targeting decorations have been introduced for BSA-GNPs, identifying the best decoration needs comprehensive investigation at the same condition. To the best of our knowledge, this is the first comprehensive *in vivo* experimental study on the different targeting decorations of BSA-GNPs to select the best one at different aspects. In this study, BSA-GNPs were decorated with three different well-known targeting agents (folic acid, glutamine, and glucose) and evaluated according to radiosensitizers determinative criteria including tumor targeting, enhancing of RT efficacy, and biocompatibility.

2. Material and methods

2.1. GNPs synthesis

All the GNPs were synthesized upon previously reported protocols with slight modifications (Jingyue and Bernd, 2015).

Bovine serum albumin-GNPs (BSA-GNPs): 2 mL aqueous solution of 50 mg/mL BSA was added to 50 mL HAuCl4 solution (1 mM) under vigorous stirring. After 10 min, NaOH solution (1 M) was added dropwise under stirring where the pH of the solution reaches to 5. Then 100 μL NaBH4 (1 wt%) was added and the mixture was continuously stirred at 60 °C for 6 h. Gradually, the color of the solution changes from light yellow to red (Singh et al., 2005). At the next step, the BSA-gold nanoparticles-folic acid (BSA-GNPs-FA), BSA-gold nanoparticles-glutamine (BSA-GNPs-Glut) and BSA-gold nanoparticles-glucose (BSA-GNPs-Glu) were synthesized. For the preparation of each suspension 100 mg glutamine, folic acid, or glucose separately was added to 15 mL of above-mentioned BSA-GNPs suspension and mixture was stirred vigorously for 12 h. Any unbound components were removed from the mixture by centrifuging the solution at 10,000 rpm for 10 min followed by three times washings with 10 mM phosphate buffer (pH = 7.1). This process was repeated three times.

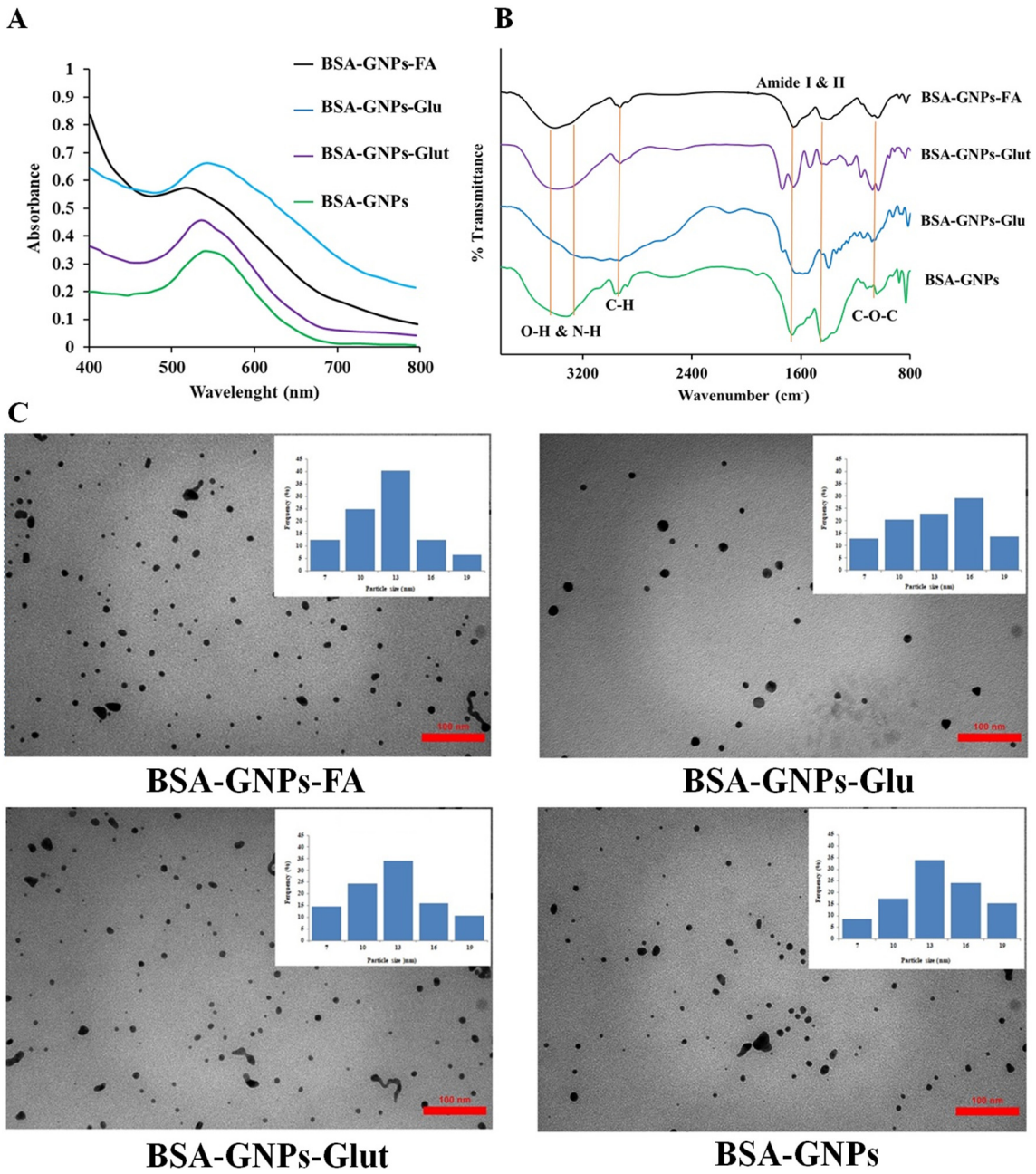

Fig. 2. Characterization of different decorations of BSA-GNPs. A) UV–Vis absorption spectra. B) The FT-IR spectra. C) TEM images and size biodistribution histograms of the GNPs.

2.2. GNPs characterizations

The UV–Vis absorbance spectra of synthesized gold nanoparticles suspensions were obtained with Shimadzu UV-160 spectrophotometer. In addition, Fourier transforms infrared spectroscopy (FT-IR) spectra were recorded using an FT-IR spectrophotometer model JASCO (Japan). All the nanoparticle suspensions were freeze-dried and FT-IR spectra were recorded. In addition, transmission electron microscopy (TEM) images were captured on a Philips EM208S 100 kV.

2.3. Cell culture

4T1 (murine mammary carcinoma) cell line was obtained from Pastor Institute of Tehran, Iran. 4T1 cells were cultured in RPMI (Sigma, USA) with 10% FBS. All cell culture mediums were supplemented with 1% penicillin, streptomycin (Sigma, USA) in a humidified atmosphere of 5% CO_2 and 95% air at 37 °C.

2.4. 4T1 breast cancer animal model

110 female BALB/c (6–8 weeks, 24 ± 2) mice were purchased from Pasteur Institute of Tehran, Iran for all the experiments. They were maintained and handled using protocols approved by guidelines of the Institutional Animal Care and Ethics Committee of Isfahan University of Medical Sciences. The animals were monitored daily to ensure clean cages, adequate food and water, and good body condition. Appropriate number of animals per cage were housed at a 12:12 h light/dark cycle. 60 number of these mice were injected with 2×10^6 cells suspended in 50 µL of DMEM-F12 into the 4th abdominal mammary fat pad subcutaneously. Animals were sacrificed if they exhibited any signs of distress like excessive weight loss (20%) or lethargy.

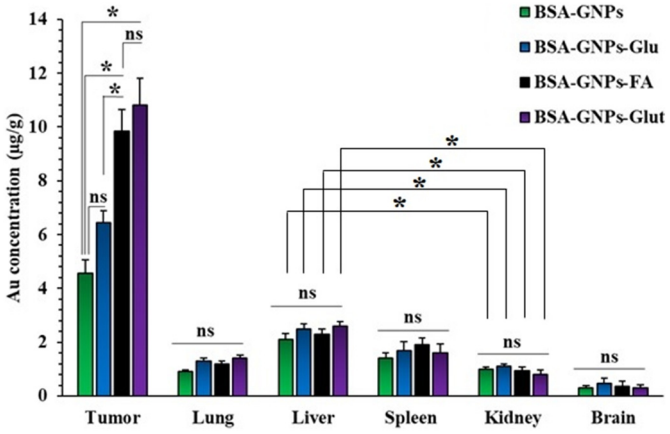

Fig. 3. Biodistribution of the BSA-GNPs, BSA-GNPs-FA, BSA-GNPs-Glu, BSA-GNPs-Glut 24 h after 10 mg/kg i.v. injection (n = 3). (*: $P < 0.05$, ns: not significant).

2.5. Inductively coupled plasma optical emission spectrometry (ICP-OES)

For assessment of the GNPs biodistribution, twelve 4T1 breast cancer-bearing mice were randomly divided in four groups (each group contained 3 mice: n = 3) and each group was injected intravenously with 10 mg/kg GNPs. Tumor, liver, kidney, spleen, lungs, and brain of the mice were harvested 24 h after injection. For measuring of gold concentration, 0.5 g of each organ was weighted and dried at 105 °C until the weight remained unchanged. The products were homogenized in powder and solved in aqua regia solution made of 12.5 M hydrochloric acid and 5 M nitric acid and maintained until the samples were completely dissolved. Gold concentration in this given volume determined by inductively coupled plasma optical emission spectrometry, ICP-OES (Varian Vista-Pro, Australia).

2.6. In vivo radiation therapy

The mice were monitored daily for growth of the implanted cancer cells and tumor formation. When the tumors became palpable, in order to determine tumors' volume, the greatest longitudinal diameter

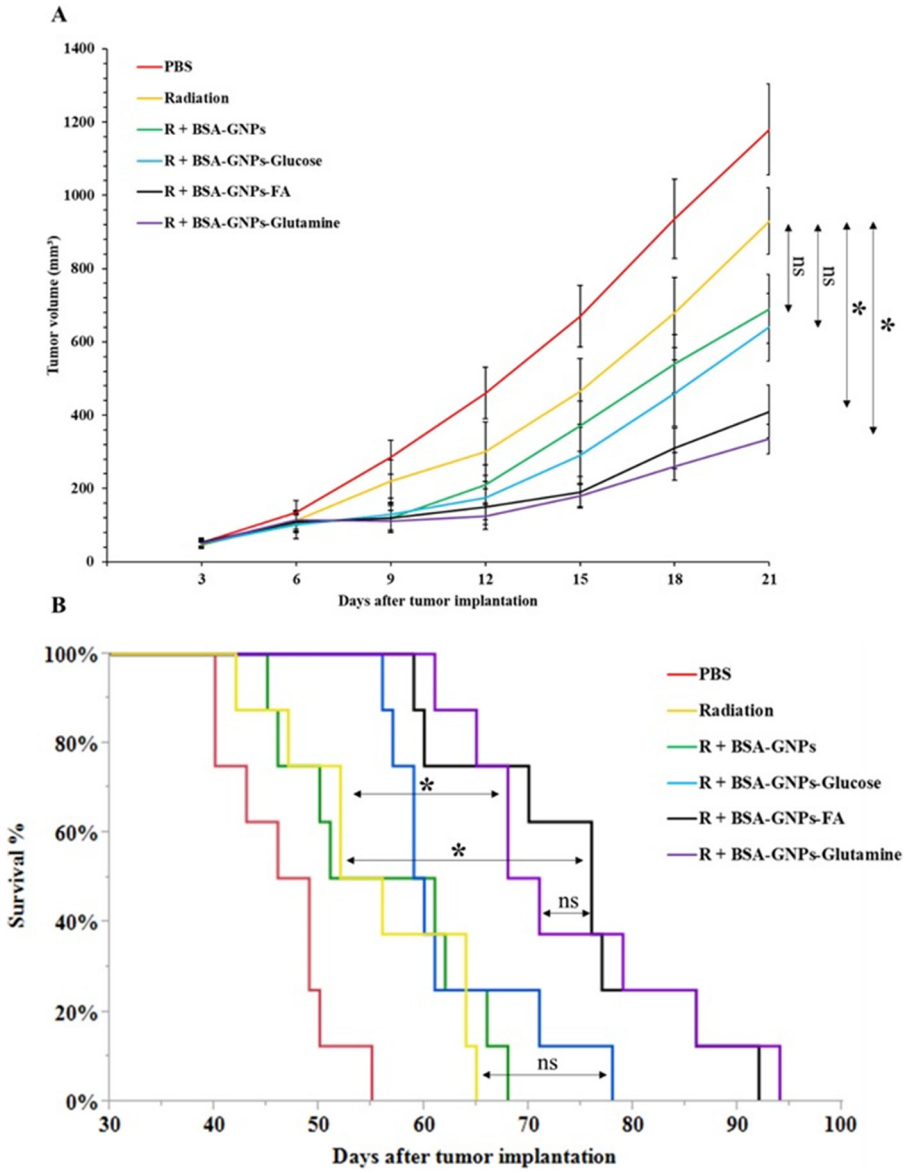

Fig. 4. BSA-GNPs, BSA-GNPs-FA, BSA-GNPs-Glu, BSA-GNPs-Glut effect on enhancement of radiation therapy efficacy for 4T1 breast tumor-bearing mice (n = 8). (*: $P < 0.05$, ns: not significant).

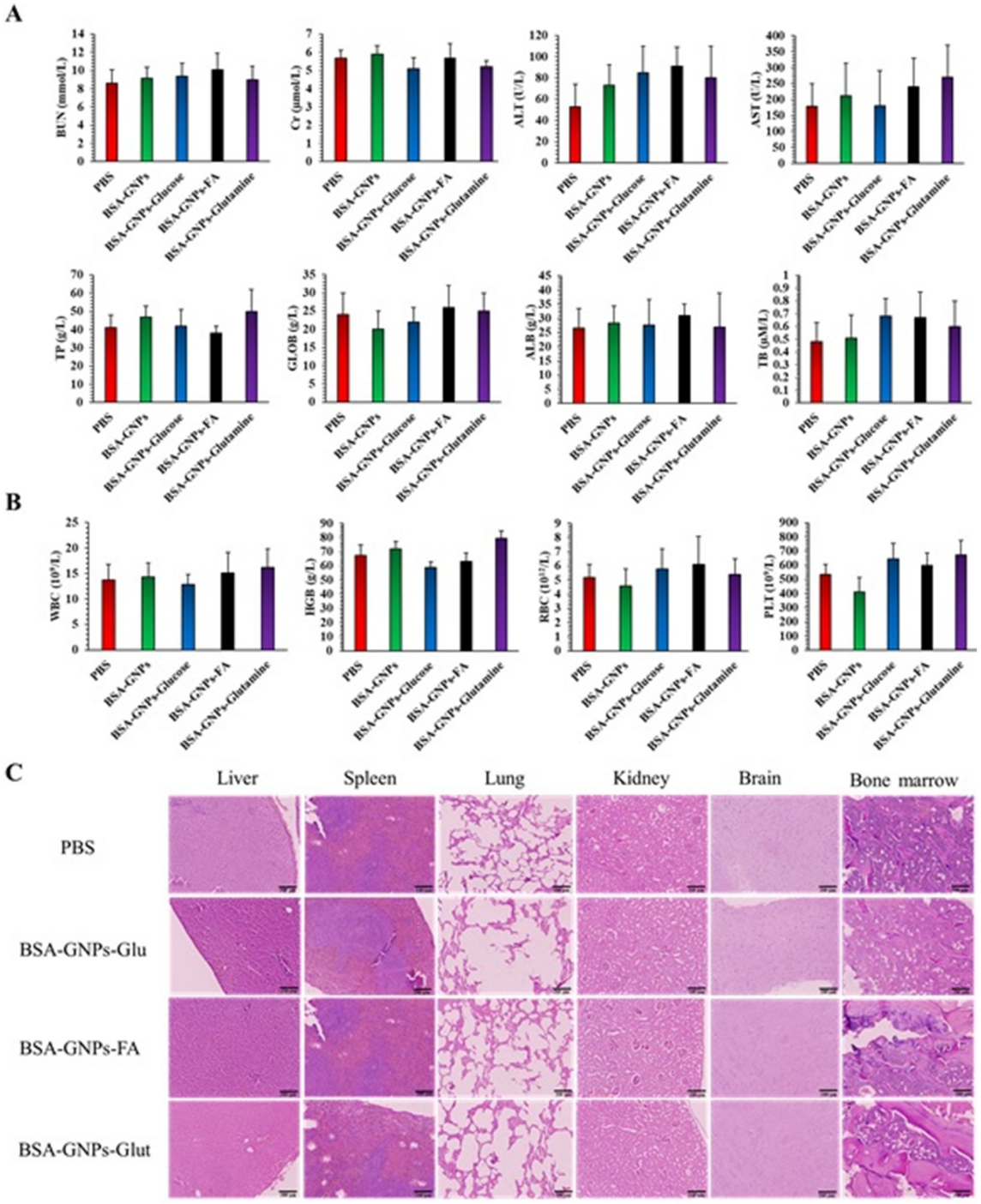

Fig. 5. Histopathological sections, blood biochemistry and hematology analyze of the mice treated with BSA-GNPs, BSA-GNPs-FA, BSA-GNPs-Glu, and BSA-GNPs-Glut 3 days after 10 mg/kg GNPs i.v. injection (n = 5). A) Blood urea nitrogen (BUN), creatinine (Cr), alanine aminotransferase (ALT), aspartate aminotransferase (AST), total protein (TP), albumin (ALB), globulin (GLOB), and total bilirubin (TB) were measured as biochemical analyzes. B) The white blood cells (WBC), red blood cells (RBC), hemoglobin (HGB), platelets (PLT) were measured as hematological analyzes. C) Histopathological sections from liver, kidney, brain, spleen, lung, and bone marrow of the mice treated with BSA-GNPs, BSA-GNPs-FA, BSA-GNPs-glucose, and BSA-GNPs-glutamine (all scale bars 200 μm).

(length) and the greatest transverse diameter (width) of the tumors were determined every day. Tumor volume based on caliper measurements were calculated by the tumor volume equation (Eq. (1)) (Faustino-Rocha et al., 2013; Jensen et al., 2008). At the 6th day after cancer cells implantation, the tumors volumes reached 70–100 mm^3. Subsequently, 48 tumor-bearing mice were randomly divided into six groups (n = 8) including PBS, Radiation therapy (RT), RT + BSA-GNPs, RT + BSA-GNPs-FA, RT + BSA-GNPs-Glu, RT + BSA-GNPs-Glut. All the GNPs were i.v. injected (10 mg/kg) 24 h pre-irradiation. Then, tumor-bearing mice were irradiated with the 6 MV X-ray using linear accelerator (Primus, Siemens Ltd, Germany). The source-to-surface distance (SSD) was 100 cm, the field size of 25 × 25 cm^2 and delivered total doses of 6 Gy with a dose rate of 200 MU/min was prepared. To minimize mice movement through irradiation, animals were anesthetized with a combination of ketamine and xylazine (Ghahremani et al., 2018a). After radiation therapy, the tumor diameters were measured with a digital caliper every 3 days and tumor volumes were calculated to evaluate the tumor growth progression at different treatment groups.

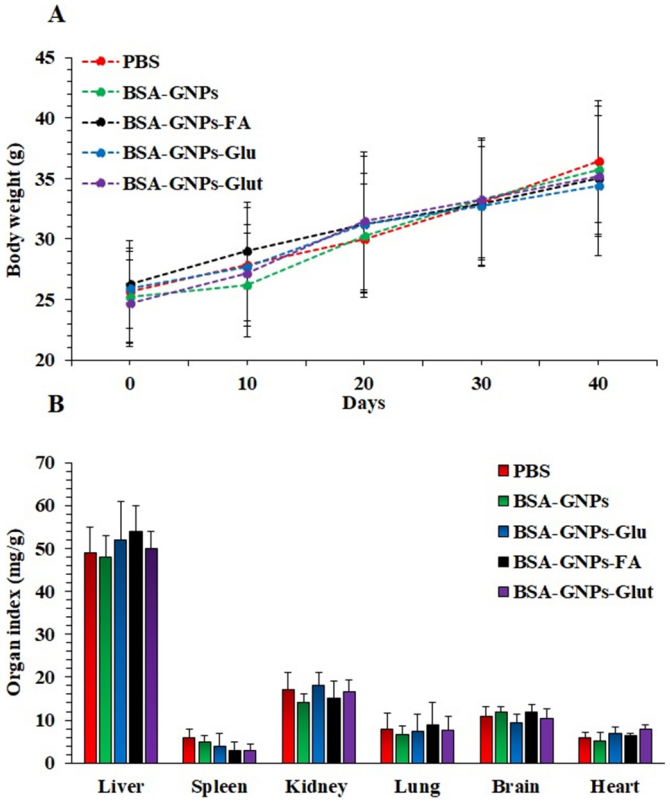

Fig. 6. Investigation of chronic toxicity of the GNPs according to A) body weight B) and organ index of BALB/c mice (n = 5) following multiple doses injection of different GNPs (10 mg/kg i.v. 2 times a week for one month).

$$\text{Tumor volume} = (\text{Tumor length}) \times (\text{Tumor width})^2/2 \quad (1)$$

2.7. Biocompatibility investigation

For evaluating organ toxicity of single dose of GNPs, 25 mice were randomly divided in 5 groups (n = 5) and then injected with 10 mg/kg of different GNPs and sacrificed after 3 days. The blood was collected for hematology analyzes (potassium EDTA collection tube) and the discarded serum (lithiumheparin collection tube) was used for biochemistry analyzes using a standard saphenous vein blood collection technique. Also, the organs were harvested for histopathological exams. The white blood cells (WBC), red blood cells (RBC), hemoglobin (HGB), platelets (PLT) were measured as hematological analyzes. Also, blood urea nitrogen (BUN), creatinine (Cr), alanine aminotransferase (ALT), aspartate aminotransferase aminotransferase (AST), total protein (TP), albumin (ALB), globulin (GLOB), and total bilirubin (TB) were measured for biochemical analyzes (Zhang et al., 2014). In addition, different organs were fixed in 10% formalin neutral buffer solution and embedded in paraffin. In the next step, dehydration was done and tissues were blocked. Thin sections about 5 μm were prepared and stained by hematoxylin and eosin. Histological photographs were obtained using a digital light microscope (Olympus, Japan) (Ghahremani et al., 2018b). Moreover, for investigation of the toxicity of multiple doses of GNPs, 25 mice were randomly divided in 5 groups (n = 5) and then were injected with the 10 mg/kg GNPs 2 times a week for one month. The mice were closely observed for any signs of toxicity within 40 days after the first injection. The animals were weighed every 10 days and visual observations for mortality, appearance, behavioral pattern changes such as weakness, aggressiveness, food or water refusal, diarrhea, salivation, discharge from eyes and ears, noisy breathing, changes in activity, clonic convulsion, anorexia, cachexia, pain or any signs of illness in each group were monitored daily (Rajeh et al., 2012). On the 40th day, all the mice were sacrificed. Vital organs such as heart, kidneys, liver, lung, brain, and spleen were autopsied and examined macroscopically for any lesions or abnormalities. Body weight and weight of the organs from the control and the treatment groups were measured and recorded. The organ indexes were calculated using the following Eq. (2) (Yang et al., 2014). All of the individual organs were observed macroscopically and their appearance was compared between both treated and control groups (Rajeh et al., 2012).

$$\frac{\textit{Organ weight (mg)}}{\textit{Body weight (g)}} = \textit{Organ index} \quad (2)$$

2.8. Statistical analysis

Statistical analyzes were performed using one-way analysis of variance (ANOVA) with Tukey's *post-hoc* test by JMP 11.0 software. The results were statistically significant at $P < 0.05$ (*: $P < 0.05$, ns: not significant). All values were expressed as the mean ± standard deviation.

3. Results and discussion

The aim of the present study is to identify the best targeting decoration of BSA-GNPs between for enhancement of breast tumor targeting and radiosensitizing efficacy. BSA-GNPs were decorated with three different targeting agents (folic acid, glucose, and glutamine) and the designed GNPs were investigated according to tumor targeting and biodistribution (Fig. 1).

3.1. Characterization of the GNPs

The GNPs characterization was done by employing UV–Vis and FT-IR analysis which are illustrated in Fig. 2. UV–Vis absorbance spectra of all prepared GNPs had maximum absorbance between 533 and 542 nm (BSA-GNPs: 539 nm, BSA-GNPs-Glut: 536 nm, BSA-GNPs-Glu: 542 nm and BSA-GNPs-FA: 533 nm). These spectra exhibited maximum absorbance wavelength shift for the BSA-GNPs after decorating with glutamine, glucose or folic acid that confirms the change in their structure (Fig. 2A). As Fig. 2B illustrates, the BSA-GNPs shows the characteristic amide I at 1680 cm^{-1} and amide II at 1500 cm^{-1}. In the BSA-GNPs-FA, BSA-GNPs-Glut, and BSA-GNPs-Glu spectra, the two characteristic amide peaks changes can exhibit the newly formed amide bond due to folic acid, glucose, and glutamine conjugation with BSA-GNPs. In addition, the changes in O—H and N—H broad stretch peaks can show the formation of new hydrogen bonds in BSA-GNPs-FA, BSA-GNPs-Glut, and BSA-GNPs-Glu spectra in comparison with BSA-GNPs. Since folic acid, glucose, and glutamine consist of amino, carboxyl, and hydroxyl groups, they can interact *via* hydrogen bonding with BSA. Also, previous studies have investigated the interaction of functional groups of these small molecules with BSA capped GNPs and introduced hydrogen bond as the main acting force between these molecules and BSA (Zhang and Jia, 2006; Li et al., 2016; Bourassa et al., 2011; Jha and Kishore, 2011; Zhang et al., 2016; Zeng et al., 2018). In addition, the TEM images and size biodistribution histograms were prepared (Fig. 2C). All the GNPs had approximately the same core shapes and size ranges between 10 and 18 nm (according to size biodistribution histograms: BSA-GNPs: 13.6 ± 3.6 nm, BSA-GNPs-Glu: 13.3 ± 3.8 nm, BSA-GNPs-FA: 12.2 ± 3.1 nm, and BSA-GNPs-Glut: 12.5 ± 3.5 nm). Therefore, different efficacies between the GNPs in the next *in vivo* evaluations can be highly attributed to their targeting decoration as they have the same core shape and size.

3.2. Biodistribution of different targeting decorations of BSA-GNPs

Radiosensitizing efficacy of GNPs is deeply dependent on the GNPs

accumulation at the tumor site. Efficient tumor targeting increase the probability of radiation beams collision with GNPs and subsequent energy deposition and cancer cells damage (Ali et al., 2017). Also, appropriate tumor targeting reduces adverse effects as a consequence of favored accumulation at target sites (Ruoslahti et al., 2010). Different studies have utilized vast variety of i.v. doses of GNPs for radiosensitizing (Zhang et al., 2015). Delivering an adequately large amount of GNPs to the tumor may be the main factor to cause significant dose enhancement. Therefore, many studies have used high dose of GNPs like 2700 mg Au/kg body weight at *in vivo* studies (Hainfeld et al., 2004). However, targeted GNPs can cause effective radiosensitization with much lower concentrations, such as 10 mg/kg (Wolfe et al., 2015). These concentrations translate into total injection doses on the order of 1 g Au for a single human treatment. These levels are likely to be suitable with regards to both toxicity and financial considerations (Schuemann et al., 2016). Also, parameters including shape, size, capping, *etc.* are determinative for tumor targeting efficacy of GNPs and some studies which have employed GNPs with approximately the same characterizations like BSA capping have reported appropriate radiation therapy enhancement by 10 mg/kg GNPs dose (Zhang et al., 2014). Therefore, 10 mg/kg was selected as the GNPs dose in this study. To evaluate biodistribution of different decoration of BSA-GNPs, 4T1 tumor-bearing mice were injected with 10 mg/kg GNPs and after 24 h, tumor, kidney, liver, spleen, lung, and brain gold contents were measured by ICP-OES (Fig. 3). Tumors exhibited significantly ($P < 0.05$) higher gold concentration in comparison with other organs for all the GNPs. BSA-GNPs-FA and BSA-GNPs-Glut exhibited the most effective tumor targeting efficacy. Folic acid and glutamine decoration of BSA-GNPs could 2.1 and 2.4 times increase BSA-GNPs tumor targeting, respectively. However, no significant difference was observed between efficacy of these two decorations for breast tumor targeting. It was interesting that glutamine and folic acid decoration caused better tumor targeting than the glucose and glucose decoration of BSA-GNPs could not significantly enhance its targeting efficacy. Although, cancer cells exhibit significantly higher glucose consumption than normal cells, most of human body cells express glucose transporters on their surface and constantly internalize glucose as the main source for energy production (Thorens and Mueckler, 2009; Barron et al., 2016). Therefore, normal cells all over the body are interested in internalization of glucose targeted nanomaterials and can decrease the amount of GNPs which will reach the tumor (Geng et al., 2014). In contrast to glucose transporters, expression of folate receptors in the most of normal tissues is low or even absent (Weitman et al., 1992; Zwicke et al., 2012; Cha et al., 2018). In addition, glutamine is a non-essential amino acid for non-proliferating normal cells and they synthesis their needed glutamine. However, cancer cells are highly dependent to exogenous glutamine and cannot proliferate or even survive in the absence of it (Zhang et al., 2017). It seems these facts can explain the lower tumoral uptake of glucose targeted GNPs when compared with the BSA-GNPs-FA and BSA-GNPs-Glut.

Hepatic and renal clearance are the two main routes of nanoparticles excretion from body (Longmire et al., 2008). Many studies have reported that nanoparticles with smaller sizes than the renal clearance barrier which is 5.5 nm can exhibit efficient renal clearance (Zhang et al., 2015; Longmire et al., 2008; Choi et al., 2007; Zhou et al., 2011). Therefore, the hepatobiliary system represents the primary route of excretion for nanoparticles > 10 nm which do not undergo renal clearance. The liver provides the critical function of catabolism and biliary excretion of these nanoparticles (Longmire et al., 2008; Choi et al., 2007). The BSA-GNPs and its different decorated GNPs size were between 10 and 18 nm. Also, as Fig. 3 illustrates, liver contained more GNPs in compassion with kidney after i.v. injection of the GNPs. Therefore, hepatic clearance is the most probable route for clearance of these nanoparticles.

3.3. Radiosensitizing efficacy of different targeting decorations of BSA-GNPs

The 4T1 syngeneic tumor model has several characteristics that make it an appropriate experimental animal model with high similarity with human mammary cancer. 4T1 tumor cells are easily transplanted into the mammary gland so the primary tumor grows in the correct anatomical site. Also, 4T1 develops spontaneous metastasis from the primary tumor and its progressive spread to lymph nodes and other organs is very similar to the human mammary cancer (Pulaski and Ostrand-Rosenberg, 2000). Moreover, 4T1 tumors exhibit high similarities with human breast tumors in histopathology (Cardiff and Wellings, 1999). Therefore, many studies have utilized this syngeneic tumor model for evaluation of different treatments' efficacies like immune therapy (Chen et al., 2007), radiation therapy (Filatenkov et al., 2014), and nanomedicine (Cun et al., 2016). In this study, for assessment of different targeting decoration effect on the radiosensitizing efficacy of BSA-GNPs, 4T1 breast tumor-bearing BALB/c mice were utilized and their tumors' growth and survival time were investigated in various treatment groups. Single dose 6 Gy MV radiation therapy was utilized as the main treatment and different targeting decorations of BSA-GNPs were injected 10 mg/kg i.v. 24 h before irradiation. As Fig. 4 illustrates, the BSA-GNPs-Glut and BSA-GNPs-FA exhibited more enhancement of radiation therapy efficacy according to better tumor growth inhibition (Fig. 4A) and significant increase of tumor-bearing mice survival in comparison with BSA-GNPs and BSA-GNPs-Glu (Fig. 4B). Mean tumor volumes of the BSA-GNPs-FA + RT and BSA-GNPs-Glut + RT groups at the last day of follow up were respectively about 40% and 50% lesser than BSA-GNPs + RT group. Also, these two groups had about 33% more mean survival time in comparison with BSA-GNPs + RT group. However, the BSA-GNPs-Glu and BSA-GNPs did not exhibit significant difference at their therapeutic efficacy. These observations are in consistency with tumor targeting assay results. As gold concentration is the main determinative factor for predicting the radiosensitizing efficacy GNPs. Glutamine and folic acid decorated BSA-GNPs exhibited the highest tumor targeting and accumulation which explains their significantly higher radiosensitizing efficacy.

3.4. Biocompatibility of different targeting decorations of BSA-GNPs

One of the main obstacles for clinical utilizing of nanomaterials is their toxicity (Anselmo and Mitragotri, 2016). Therefore, exact evaluation of organ toxicity of nanomaterials is very important. The GNPs were injected (10 mg/kg i.v.) to BALB/c mice and the animals were sacrificed after 3 days to investigate the toxicity of single dose of the GNPs. Their blood and plasma were collected for biochemical (Fig. 5A) and hematological (Fig. 5B) analyzes and, the organs histopathological exams were done (Fig. 5C). Additionally, as the clinical application would include multiple episodes of treatment over time, toxicity of multiple doses of the GNPs was investigated. Therefore, BALB/c mice were i.v. injected with 10 mg/kg GNPs 2 times a week for one month and general parameters including appearance, behavioral pattern, food intake (Table 1S), body weight, and organ index were evaluated for 40 days after the first injection (Fig. 6). No sign of changes at the appearance and behavioral pattern of the mice after multiple doses injection of different GNPs were observed (Table 1S). Also, the food consumption, body weight, and organ index of each animal during the entire experimental period were evaluated according to previous studies (Kim et al., 2008; De Jong et al., 2013; Yang et al., 2017). No significant changes in food consumption and body weight were observed in either of the treatment and control groups. As shown in Fig. 6A, the mice body weight of the GNPs-treated and control groups displayed similar increasing trends. The liver, kidney, heart, spleen, brain, and lungs exhibited no significant differences in mass in comparison with the control and their macroscopic evaluations were completely normal. Therefore, single and multiple i.v. injection doses of

these decorations of the BSA-GNPs are safe.

4. Conclusions

Cancer cells specific gold nanoparticles, especially BSA-GNPs are gaining lots of attention for enhancement of tumor radiation therapy efficacy as radiosensitizers. GNPs targeting decoration is significantly determinative for their tumor targeting efficacy. Therefore, many effective decorations for enhancement of GNPs efficacy have been introduced. However, a comprehensive study for selection of the best decoration can be helpful. In the present study, three well-known targeting agents (folic acid, glucose, and glutamine) for the decoration of BSA-GNPs were evaluated according to tumor targeting, biodistribution, biocompatibility, and enhancement of radiation therapy. BSA-GNPs decoration with glutamine and folic acid as targeting agents significantly enhances their efficacy which is obviously related to tumor targeting.

Supplementary data to this article can be found online at https://doi.org/10.1016/j.ejps.2019.01.037.

Acknowledgement

The authors gratefully acknowledge the support of this study by the Research Council of University of Isfahan and financial support of the project by Iran National Science Foundation (INSF, Grant No. 93031920).

Conflict of interests

The authors declare that they have no competing interests.

References

Ali, M., Pandey, R.K., Khatoon, N., Narula, A., Mishra, A., Prajapati, V.K., 2017. Exploring dengue genome to construct a multi-epitope based subunit vaccine by utilizing immunoinformatics approach to battle against dengue infection. Sci. Rep. 7 (1), 9232.
Anselmo, A.C., Mitragotri, S., 2016. Nanoparticles in the clinic. Bioeng. Transl. Med. 1 (1), 10–29.
Barron, C.C., Bilan, P.J., Tsakiridis, T., Tsiani, E., 2016. Facilitative glucose transporters: implications for cancer detection, prognosis and treatment. Metabolism 65 (2), 124–139.
Baskar, R., Lee, K.A., Yeo, R., Yeoh, K.-W., 2012. Cancer and radiation therapy: current advances and future directions. Int. J. Med. Sci. 9 (3), 193.
Bourassa, P., Hasni, I., Tajmir-Riahi, H.J., 2011. Folic acid complexes with human and bovine serum albumins. Food Chem. 129 (3), 1148–1155.
Brown, R., Corde, S., Oktaria, S., Konstantinov, K.K., Rosenfeld, A.B., Lerch, M.L., Tehei, M., 2017. Nanostructures, Concentrations and Energies: An Ideal Equation to Extend Therapeutic Efficiency on Radioresistant 9L Tumour Cells Using Ta2O5 Ceramic Nanostructured Particles.
Butterworth, K.T., McMahon, S.J., Currell, F.J., Prise, K.M., 2012. Physical basis and biological mechanisms of gold nanoparticle radiosensitization. Nanoscale 4 (16), 4830–4838.
Cardiff, R.D., Wellings, S.R., 1999. The comparative pathology of human and mouse mammary glands. J. Mammary Gland Biol. Neoplasia 4 (1), 105–122.
Cha, Y., Kim, E.-S., Koo, J., 2018. Amino acid transporters and glutamine metabolism in breast cancer. Int. J. Mol. Sci. 19 (3), 907.
Chen, L., Huang, T.-G., Meseck, M., Mandeli, J., Fallon, J., Woo, S.L., 2007. Rejection of metastatic 4T1 breast cancer by attenuation of Treg cells in combination with immune stimulation. Mol. Ther. 15 (12), 2194–2202.
Choi, H.S., Liu, W., Misra, P., Tanaka, E., Zimmer, J.P., Ipe, B.I., Bawendi, M.G., Frangioni, J.V., 2007. Renal clearance of quantum dots. Nat. Biotechnol. 25 (10), 1165.
Cun, X., Ruan, S., Chen, J., Zhang, L., Li, J., He, Q., Gao, H., 2016. A dual strategy to improve the penetration and treatment of breast cancer by combining shrinking nanoparticles with collagen depletion by losartan. Acta Biomater. 31, 186–196.
De Jong, W.H., Van Der Ven, L.T., Sleijffers, A., Park, M.V., Jansen, E.H., Van Loveren, H., Vandebriel, R.J., 2013. Systemic and immunotoxicity of silver nanoparticles in an intravenous 28 days repeated dose toxicity study in rats. Biomaterials 34 (33), 8333–8343.
Faustino-Rocha, A., Oliveira, P.A., Pinho-Oliveira, J., Teixeira-Guedes, C., Soares-Maia, R., Da Costa, R.G., Colaco, B., Pires, M.J., Colaço, J., Ferreira, R.J., 2013. Estimation of rat mammary tumor volume using caliper and ultrasonography measurements. Lab. Anim. 42 (6), 217.
Filatenkov, A., Baker, J., Müller, A.M., Ahn, G.-O., Kohrt, H., Dutt, S., Jensen, K., Dejbakhsh-Jones, S., Negrin, R.S., Shizuru, J.A., 2014. Treatment of 4T1 metastatic breast cancer with combined hypofractionated irradiation and autologous T-cell infusion. Radiat. Res. 182 (2), 163–169.
Geng, F., Xing, J.Z., Chen, J., Yang, R., Hao, Y., Song, K., Kong, B., 2014. Pegylated glucose gold nanoparticles for improved in-vivo bio-distribution and enhanced radiotherapy on cervical cancer. J. Biomed. Nanotechnol. 10 (7), 1205–1216.
Ghahremani, F., Shahbazi-Gahrouei, D., Kefayat, A., Motaghi, H., Mehrgardi, M.A., Javanmard, S.H., 2018a. AS1411 aptamer conjugated gold nanoclusters as a targeted radiosensitizer for megavoltage radiation therapy of 4T1 breast cancer cells. RSC Adv. 8 (8), 4249–4258.
Ghahremani, F., Kefayat, A., Shahbazi-Gahrouei, D., Motaghi, H., Mehrgardi, M.A., Haghjooy-Javanmard, S.J., 2018b. AS1411 aptamer-targeted gold nanoclusters effect on the enhancement of radiation therapy efficacy in breast tumor-bearing mice. Nanomedicine 13 (20), 2563–2578.
Hainfeld, J.F., Slatkin, D.N., Smilowitz, H.M., 2004. The use of gold nanoparticles to enhance radiotherapy in mice. Phys. Med. Biol. 49 (18), N309.
Hamanaka, R.B., Chandel, N.S., 2012. Targeting glucose metabolism for cancer therapy. J. Exp. Med. 209 (2), 211–215.
Hartmann, L.C., Keeney, G.L., Lingle, W.L., Christianson, T.J., Varghese, B., Hillman, D., Oberg, A.L., Low, P.S., 2007. Folate receptor overexpression is associated with poor outcome in breast cancer. Int. J. Cancer 121 (5), 938–942.
Haume, K., Rosa, S., Grellet, S., Śmiałek, M.A., Butterworth, K.T., Solov'yov, A.V., Prise, K.M., Golding, J., Mason, N.J., 2016. Gold nanoparticles for cancer radiotherapy: a review. Cancer Nanotechnol. 7 (1), 8.
Jain, S., Coulter, J.A., Hounsell, A.R., Butterworth, K.T., McMahon, S.J., Hyland, W.B., Muir, M.F., Dickson, G.R., Prise, K.M., Currell, F.J., 2011. Cell-specific radiosensitization by gold nanoparticles at megavoltage radiation energies. Int. J. Radiat. Oncol. Biol. Phys. 79 (2), 531–539.
Jensen, M.M., Jørgensen, J.T., Binderup, T., Kjær, A.J., 2008. Tumor volume in subcutaneous mouse xenografts measured by microCT is more accurate and reproducible than determined by 18 F-FDG-microPET or external caliper. BMC Med. Imaging 8 (1), 16.
Jha, N.S., Kishore, N., 2011. Thermodynamic studies on the interaction of folic acid with bovine serum albumin. J. Chem. Thermodyn. 43 (5), 814–821.
Jingyue, Z., Bernd, F., 2015. Synthesis of gold nanoparticles via chemical reduction methods. In: Proceedings of the Nanocon, Brno, Czech Republic, pp. 14–16.
Khullar, P., Singh, V., Mahal, A., Dave, P.N., Thakur, S., Kaur, G., Singh, J., Singh Kamboj, S., Singh Bakshi, M., 2012. Bovine serum albumin bioconjugated gold nanoparticles: synthesis, hemolysis, and cytotoxicity toward cancer cell lines. J. Phys. Chem. C 116 (15), 8834–8843.
Kim, Y.S., Kim, J.S., Cho, H.S., Rha, D.S., Kim, J.M., Park, J.D., Choi, B.S., Lim, R., Chang, H.K., Chung, Y.H., 2008. Twenty-eight-day oral toxicity, genotoxicity, and gender-related tissue distribution of silver nanoparticles in Sprague-Dawley rats. Inhal. Toxicol. 20 (6), 575–583.
Ko, Y.-H., Lin, Z., Flomenberg, N., Pestell, R.G., Howell, A., Sotgia, F., Lisanti, M.P., Martinez-Outschoorn, U.E., 2011. Glutamine fuels a vicious cycle of autophagy in the tumor stroma and oxidative mitochondrial metabolism in epithelial cancer cells: implications for preventing chemotherapy resistance. Cancer Biol. Ther. 12 (12), 1085–1097.
Li, H., Cheng, Y., Liu, Y., Chen, B.J., 2016. Fabrication of folic acid-sensitive gold nanoclusters for turn-on fluorescent imaging of overexpression of folate receptor in tumor cells. Talanta 158, 118–124.
Longmire, M., Choyke, P.L., Kobayashi, H., 2008. Clearance Properties of Nano-sized Particles and Molecules as Imaging Agents: Considerations and Caveats.
Lu, W., Pelicano, H., Huang, P., 2010. Cancer metabolism: is glutamine sweeter than glucose? Cancer Cell 18 (3), 199–200.
Maddalena, F., Lettini, G., Gallicchio, R., Sisinni, L., Simeon, V., Nardelli, A., Venetucci, A.A., Storto, G., Landriscina, M., 2015. Evaluation of glucose uptake in normal and cancer cell lines by positron emission tomography. Mol. Imaging 14 (9) (7290.2015.00021).
Malik, A., Sultana, M., Qazi, A., Qazi, M.H., Parveen, G., Waquar, S., Ashraf, A.B., Rasool, M., 2016. Role of natural radiosensitizers and cancer cell radioresistance: an update. Anal. Cell. Pathol. 2016.
McQuaid, H.N., Muir, M.F., Taggart, L.E., McMahon, S.J., Coulter, J.A., Hyland, W.B., Jain, S., Butterworth, K.T., Schettino, G., Prise, K.M., 2016. Imaging and radiation effects of gold nanoparticles in tumour cells. Sci. Rep. 6, 19442.
Miranda, É.G., Tofanello, A., Brito, A.M., Lopes, D.M., Albuquerque, L.J., de Castro, C.E., Costa, F.N., Giacomelli, F.C., Ferreira, F.F., Araújo-Chaves, J.C., 2016. Effects of gold salt speciation and structure of human and bovine serum albumins on the synthesis and stability of gold nanostructures. Front. Chem. 4.
Mocan, L., Matea, C., Tabaran, F.A., Mosteanu, O., Pop, T., Mocan, T., Iancu, C., 2015. Photothermal treatment of liver cancer with albumin-conjugated gold nanoparticles initiates Golgi Apparatus–ER dysfunction and caspase-3 apoptotic pathway activation by selective targeting of Gp60 receptor. Int. J. Nanomedicine 10, 5435.
Murawala, P., Tirmale, A., Shiras, A., Prasad, B., 2014. In situ synthesized BSA capped gold nanoparticles: effective carrier of anticancer drug methotrexate to MCF-7 breast cancer cells. Mater. Sci. Eng. C 34, 158–167.
Nicol, J.R., Dixon, D., Coulter, J.A., 2015. Gold nanoparticle surface functionalization: a necessary requirement in the development of novel nanotherapeutics. Nanomedicine 10 (8), 1315–1326.
Patil, Y., Amitay, Y., Ohana, P., Shmeeda, H., Gabizon, A., 2016. Targeting of pegylated liposomal mitomycin-C prodrug to the folate receptor of cancer cells: intracellular activation and enhanced cytotoxicity. J. Control. Release 225, 87–95.
Pavlova Natalya, N., Thompson Craig, B., 2016. The emerging hallmarks of cancer metabolism. Cell Metab. 23 (1), 27–47.
Pulaski, B.A., Ostrand-Rosenberg, S., 2000. Mouse 4T1 breast tumor model. Curr. Protoc. Immunol. 39 (1), 20–22.

Rajeh, M.A.B., Kwan, Y.P., Zakaria, Z., Latha, L.Y., Jothy, S.L., Sasidharan, S.J., 2012. Acute toxicity impacts of *Euphorbia hirta* L extract on behavior, organs body weight index and histopathology of organs of the mice and *Artemia salina*. Pharm. Res. 4 (3), 170.
Reddy, J.A., Low, P.S., 1998. Folate-mediated targeting of therapeutic and imaging agents to cancers. Crit. Rev. Ther. Drug Carrier Syst. 15 (6).
Ruoslahti, E., Bhatia, S.N., Sailor, M.J., 2010. Targeting of drugs and nanoparticles to tumors. J. Cell Biol. 188 (6), 759–768.
Schuemann, J., Berbeco, R., Chithrani, D.B., Cho, S.H., Kumar, R., McMahon, S.J., Sridhar, S., Krishnan, S., 2016. Roadmap to clinical use of gold nanoparticles for radiation sensitization. Int. J. Radiat. Oncol. Biol. Phys. 94 (1), 189–205.
Singh, S., 2017. Glucose decorated gold nanoclusters: a membrane potential independent fluorescence probe for rapid identification of cancer cells expressing Glut receptors. Colloids Surf. B: Biointerfaces 155, 25–34.
Singh, A.V., Bandgar, B.M., Kasture, M., Prasad, B., Sastry, M., 2005. Synthesis of gold, silver and their alloy nanoparticles using bovine serum albumin as foaming and stabilizing agent. J. Mater. Chem. 15 (48), 5115–5121.
Su, X.-Y., Liu, P.-D., Wu, H., Gu, N., 2014. Enhancement of radiosensitization by metal-based nanoparticles in cancer radiation therapy. Cancer Biol. Med. 11 (2), 86.
Thorens, B., Mueckler, M., 2009. Glucose transporters in the 21st century. 298 (2), E141–E145.
Toffoli, G., Cernigoi, C., Russo, A., Gallo, A., Bagnoli, M., Boiocchi, M., 1997. Overexpression of folate binding protein in ovarian cancers. Int. J. Cancer 74 (2), 193–198.
Tse, W.H., Gyenis, L., Litchfield, D.W., Zhang, J., 2017. Cellular interaction influenced by surface modification strategies of gelatin-based nanoparticles. J. Biomater. Appl. 31 (7), 1087–1096.
Vander Heiden, M.G., Cantley, L.C., Thompson, C.B., 2009. Understanding the Warburg effect: the metabolic requirements of cell proliferation. Science 324 (5930), 1029–1033.
Venturelli, L., Nappini, S., Bulfoni, M., Gianfranceschi, G., Dal Zilio, S., Coceano, G., Del Ben, F., Turetta, M., Scoles, G., Vaccari, L., 2016. Glucose is a key driver for GLUT1-mediated nanoparticles internalization in breast cancer cells. Sci. Rep. 6, 21629.
Weitman, S.D., Lark, R.H., Coney, L.R., Fort, D.W., Frasca, V., Zurawski, V.R., Kamen, B.A., 1992. Distribution of the folate receptor GP38 in normal and malignant cell lines and tissues. Cancer Res. 52 (12), 3396–3401.
Wessler, S., Aberger, F., Hartmann, T.N., 2017. The sound of tumor cell-microenvironment communication–composed by the Cancer Cluster Salzburg research network. Cell Commun. Signal 15 (1), 20.
Wise, D.R., Thompson, C.B., 2010. Glutamine addiction: a new therapeutic target in cancer. Trends Biochem. Sci. 35 (8), 427–433.
Wolfe, T., Chatterjee, D., Lee, J., Grant, J.D., Bhattarai, S., Tailor, R., Goodrich, G., Nicolucci, P., Krishnan, S., 2015. Targeted gold nanoparticles enhance sensitization of prostate tumors to megavoltage radiation therapy in vivo. Nanomedicine 11 (5), 1277–1283.
Yang, Y., Lan, J., Xu, Z., Chen, T., Zhao, T., Cheng, T., Shen, J., Lv, S., Zhang, H.J., 2014. Toxicity and biodistribution of aqueous synthesized ZnS and ZnO quantum dots in mice. Nanotoxicology 8 (1), 107–116.
Yang, L., Kuang, H., Zhang, W., Aguilar, Z.P., Wei, H., Xu, H., 2017. Comparisons of the biodistribution and toxicological examinations after repeated intravenous administration of silver and gold nanoparticles in mice. Sci. Rep. 7 (1), 3303.
Younes, M., Brown, R.W., Stephenson, M., Gondo, M., Cagle, P.T., 1997. Overexpression of Glut1 and Glut3 in stage I nonsmall cell lung carcinoma is associated with poor survival. Cancer 80 (6), 1046–1051.
Zeng, Y., Chang, Y.H., Gharib, M., Parak, W.J., Chakraborty, I., 2018. Understanding the interaction of glutamate salts with serum albumin protected prism-shaped silver nanoparticles toward glutamate sensing. Part. Part. Syst. Charact. 36 (1), 1–5 (1800229).
Zhang, A., Jia, L.J., 2006. Spectroscopic study of the interaction between folic acid and bovine serum albumin. Spectrosc. Lett. 39 (4), 285–298.
Zhang, X.D., Chen, J., Luo, Z., Wu, D., Shen, X., Song, S.S., Sun, Y.M., Liu, P.X., Zhao, J., Huo, S.J., 2014. Enhanced tumor accumulation of sub-2 nm gold nanoclusters for cancer radiation therapy. Adv. Healthc. Mater. 3 (1), 133–141.
Zhang, X.-D., Luo, Z., Chen, J., Song, S., Yuan, X., Shen, X., Wang, H., Sun, Y., Gao, K., Zhang, L., 2015. Ultrasmall glutathione-protected gold nanoclusters as next generation radiotherapy sensitizers with high tumor uptake and high renal clearance. Sci. Rep. 5, 8669.
Zhang, Q., Ni, Y., Kokot, S., 2016. Competitive interactions between glucose and lactose with BSA: which sugar is better for children? Analyst 141 (7), 2218–2227.
Zhang, J., Pavlova, N.N., Thompson, C.B., 2017. Cancer cell metabolism: the essential role of the nonessential amino acid, glutamine. EMBO J. 36 (10), 1302–1315.
Zhou, C., Long, M., Qin, Y., Sun, X., Zheng, J., 2011. Luminescent gold nanoparticles with efficient renal clearance. Angew. Chem. 123 (14), 3226–3230.
Zwicke, G.L., Mansoori, G., Jeffery, C.J., 2012. Utilizing the folate receptor for active targeting of cancer nanotherapeutics. Nano Rev. 3 (1), 18496.